Journal of Materials Chemistry

Cite this: J. Mater. Chem., 2012, 22, 14085

www.rsc.org/materials

PAPER

Resistive switching non-volatile and volatile memory behavior of aromatic polyimides with various electron-withdrawing moieties†

Chih-Jung Chen,[a] Hung-Ju Yen,[a] Wen-Chang Chen[ab] and Guey-Sheng Liou*[a]

Received 6th April 2012, Accepted 18th May 2012
DOI: 10.1039/c2jm32155f

In this study, *N*,*N*′-bis(4-aminophenyl)-*N*,*N*′-di(4-methoxyl-phenyl)1,4-phenylenediamine [$(OMe)_2$TPPA-diamine] and various dianhydrides such as oxydiphthalic dianhydride (ODPA), 3,3′,4,4′-diphenylsulfonetetracarboxylic dianhydride (DSDA), pyromellitic dianhydride (PMDA), and 1,4,5,8-naphthalenetetracarboxylic dianhydride (NPDA) were used to synthesize new functional polyimides $(OMe)_2$TPPA-ODPI (**ODPI**), $(OMe)_2$TPPA-DSPI (**DSPI**), $(OMe)_2$TPPA-PMPI (**PMPI**), and $(OMe)_2$TPPA-NPPI (**NPPI**), respectively for memory device applications. For comparison, the corresponding $(OMe)_2$TPPA-6FPI (**6FPI**) was also added into the discussion. The differences of HOMO energy levels, LUMOs energy levels, and dipole moment among these five polyimides with different electron-withdrawing linkage were investigated and demonstrated the effect on the memory behavior. With the electron-withdrawing moiety intensity of polyimides increasing, the retention time of corresponding memory device increases. **ODPI** didn't have memory properties, **6FPI** exhibited DRAM characteristic, and **PMPI** with stronger electron-withdrawing linkage revealed SRAM behavior. **NPPI** with the strongest electron-withdrawing linkage showed WORM type non-volatile memory behavior. Interestingly, **DSPI** have the LUMO energy levels between **6FPI** and **PMPI** but revealed non-volatile WORM behavior resulting from the highest dipole moment 5.45 D.

Introduction

Bistable resistive switching polymeric materials[1] have been investigated for the past three decades since the first polymer electronic memories were reported by Sliva *et al.*[1j] in 1970. In addition to memory devices, the use of polymeric materials in other electronic devices also attracted significant attention, such as light-emitting devices,[2] transistors,[3] and solar cells[4] resulting from the advantages of rich structural flexibility, low-cost, solution processability, and three-dimensional stacking capability.[5] As compared to the traditional inorganic memory materials, polymeric memory materials store information in the form of high (ON) and low (OFF) current state in place of the amount of charges stored in a cell in silicon devices. In the starting stage of polymer memory applications, polymers were used as polyelectrolytes[6] and matrices in a doped system.[1f,7] To advance the function of polymers for memory devices further, the design and synthesis of polymers with specific structures that can provide the expected memory properties within a single polymer chain is an important and crucial issue.

Donor–acceptor type polymers contain both electron donor and acceptor moieties within a repeating unit, which can contribute electronic transition between the ground and excited states and exhibited memory behavior. Aromatic polyimides are promising candidates for memory device applications[8] among all the studied donor–acceptor systems because of their excellent thermal dimensional stability, chemical resistant, and high ON/OFF current ratio resulting from the low conductivity in the OFF state.[9] The introduction of triphenylamine (TPA) group into polyimide could improve the solubility of polymer and enhance the solution processability.[10,11] The TPA based polyimides 6F-TPA PI[8a] used by Kang and co-workers demonstrated electrical switching behavior and indicated as volatile dynamic random access memory (DRAM).[8b] Then, a series of TPA-based polyimides with different substituted groups were prepared for memory devices, such as 4-hydroxy-substituted TPA-based polyimide (6F-HTPA PI)[8e] and 4-(*N*,*N*-diphenylamine)-substituted TPA-based polyimide (6F-2TPA PI)[8g] exhibited non-volatile write-once-read-many-times (WORM) properties and non-volatile WORM or volatile DRAM characteristics depending on the thickness of polymer films, respectively. The diverse memory properties of TPA-based polyimides with different substituted groups imply the importance of electron donating moieties. In this study, $(OMe)_2$TPPA moiety was chosen as an electron donor. Comparing to 2TPA, $(OMe)_2$TPPA

[a]*Functional Polymeric Materials Laboratory, Institute of Polymer Science and Engineering, National Taiwan University, 1 Roosevelt Road, 4th Sec., Taipei 10617, Taiwan. E-mail: gsliou@ntu.edu.tw*
[b]*Department of Chemical Engineering, National Taiwan University, 1 Roosevelt Road, 4th Sec., Taipei 10617, Taiwan*

† Electronic supplementary information (ESI) available: IR spectra of polyimides films and memory device characteristics of Au/DSPI/Au. See DOI: 10.1039/c2jm32155f

has two electroactive nitrogen atoms in the main chain with substituted electron-donating methoxy groups which results in not only a higher HOMO energy level which has been considered as a contribution for the lower switching-on voltage but also increasing device lifetime due to the stabilized cationic radical after oxidation.[10c,11]

In addition to structural effect of the electron-donor, the difference of electrical switching behavior for DRAM and static random access memory (SRAM) can also be induced by introduction of different linkage groups between the electron donor and the electron accepter moieties.[8i,k,m] The conformational changes between the donor and acceptor moiety induced by charge transfer could increase the torsional displacement and produce a potential energy barrier for the CT complex relaxing to the original state. As a result, the retention time for the polymer memory device maintaining at ON state should be longer after removing the applying electric field. Thus, the obtaining polymer memory device could reveal SRAM type memory behavior. Besides, the dipole moment also manifested significant effect on memory properties. According to reported literature, higher dipole moment of the donor–acceptor polymer structures brought to a more stable CT complex and increased ON state retention time of memory device when the applied power was removed.[1c,8j,k] By increasing the dipole moment effect, polymer memory properties can transit from DRAM to SRAM and even become WORM type or flash type non-volatile memory behavior.

Polyimides synthesized from different kinds of dianhydrides (acceptors) having different LUMO energy levels, electron-withdrawing ability, and dipole moment should reveal anomalous properties for polymer memory devices. There are some references which mention polyimides synthesized from different dianhydrides for memory devices.[8p,q] However, to the best of our knowledge, the effects of different dianhydrides (electron accepter) within the polyimide backbone on memory properties have not been investigated in detail and systematically to date. Therefore, we utilized electron-donating *N*,*N*′-bis(4-aminophenyl)-*N*,*N*′-di(4-methoxylphenyl)1,4-phenylenediamine [$(OMe)_2$TPPA-diamine][11] and dianhydrides having different electron-withdrawing capability such as oxydiphthalic dianhydride (ODPA), 3,3′,4,4′-diphenylsulfonetetracarboxylic dianhydride (DSDA), pyromellitic dianhydride (PMDA), and 1,4,5,8-naphthalenetetracarboxylic dianhydrides (NPDA), respectively, to synthesize these new functional polyimides $(OMe)_2$TPPA-ODPI (**ODPI**), $(OMe)_2$TPPA-DSPI (**DSPI**), $(OMe)_2$TPPA-PMPI (**PMPI**), and $(OMe)_2$TPPA-NPPI (**NPPI**). For comparison, the corresponding $(OMe)_2$TPPA-6FPI (**6FPI**) published before was also added into the discussion in this study.[8m] The obtained $(OMe)_2$TPPA-containing polyimides **ODPI**, **DSPI**, and **NPPI** are solution-processable and could be readily cast into smooth films by spin coating. These polymer memory devices were fabricated with the sandwich configuration of ITO/polymer/Al as shown in Fig. 1, and the memory properties were characterized by *I*–*V* measurements. In order to investigate switching mechanism of the memory devices, molecular simulation on the basic unit was carried out by DFT/B3LYP/6-31G(d) with the Gaussian 09 program, and the difference of dipole moment, HOMO energy level, and LUMOs energy level among these polyimides was demonstrated to affect the volatile memory behavior.

Results and discussion

Synthesis and characterization of the polyimides

ODPI and **DSPI** were prepared in a conventional two-step procedure by the reaction of equal molar amounts of diamine (**1**)[11] with commercially available aromatic tetracarbonxylic dianhydrides ODPA (**2**) and DSDA (**4**) in NMP at room temperature to form precursor poly(amic acid)s, followed by chemical imidization, as shown in Scheme 1. Synthesis and characterization of the **6FPI** has been described previously.[8m] **PMPI** was prepared by the reaction of diamine (**1**) with a commercially available dianhydride PMDA (**5**) in DMAc at room temperature to obtain the precursor poly(amic acid), followed by thermal imidization. A one-step method was utilized to prepare **NPPI** in *m*-cresol. The photographs shown in Scheme 1 reveal the appearance and color of these flexible or free-standing polyimide films. The films exhibit obviously darker color when the electron withdrawing ability of dianhydrides increase due to the stronger charge-transfer effect between TPPA and phthalic imide ring which can also be manifested by cyclic voltammetry experiments, UV-vis absorption spectra, and Gaussian simulation results. The inherent viscosity and GPC analysis data of the TPPA series polyimides are summarized in Table 1. The ^{1}H NMR spectrum of **DSPI** (DMSO-d_6, δ, ppm) was used as a representative example to confirm the resulting polyimide structure as shown in Fig. 2, and the peaks could be assigned as 3.69 (s, 6H, $-OCH_3$), 6.9–7.19 (m, 22H), 8.10 (d, 2H), and 8.54 (d, 4H). The formation of polyimides was also demonstrated by IR spectra summarized in Fig. S1–S4.† Anal. calcd (%) for **DSPI** were C, 69.89; H, 3.91; N, 6.79; S, 3.89 and found C, 68.62; H, 4.40; N, 6.86; S, 3.72.

Thermal properties and solubility behavior of the polyimides

The thermal properties of TPPA series polyimides were investigated by TGA and DSC, and the results are summarized in Table 2. Typical TGA curves of these polyimides in both air and nitrogen atmospheres are shown in Fig. 3. The 10% weight-loss temperatures of the polyimides in nitrogen and air were recorded in the range of 490–570 °C and 490–560 °C, respectively. The amounts of carbonized residue (char yield) of TPPA series polyimides in nitrogen atmosphere were in the range 57–64% at 800 °C, which could be ascribed to their high aromatic content. The glass transition temperatures T_g were in the range 284–296 °C except for 245 °C of **ODPI** resulting from the flexible ether linkage. The solubility behavior of TPPA series polyimides were investigated qualitatively and the results are listed in Table 3. The polyimides **ODPI**, **6FPI**, and **DSPI** exhibited excellent solubility not only in polar aprotic organic solvents such as NMP, DMAc, and DMF, but also in less polar solvent such as $CHCl_3$. The excellent solubility can be attributed to the existence of the bulky TPPA which limit the intermolecular interactions. This excellent solubility is conducive to fabricate memory device by solution process. **NPPI** only dissolved in *m*-cresol on heating, and *m*-cresol was utilized to prepare NPPI memory device. Memory devices of **PMPI** was prepared by poly(amic acid) solution and converted into polyimides *via* thermal imidization because of the solubility limitation.

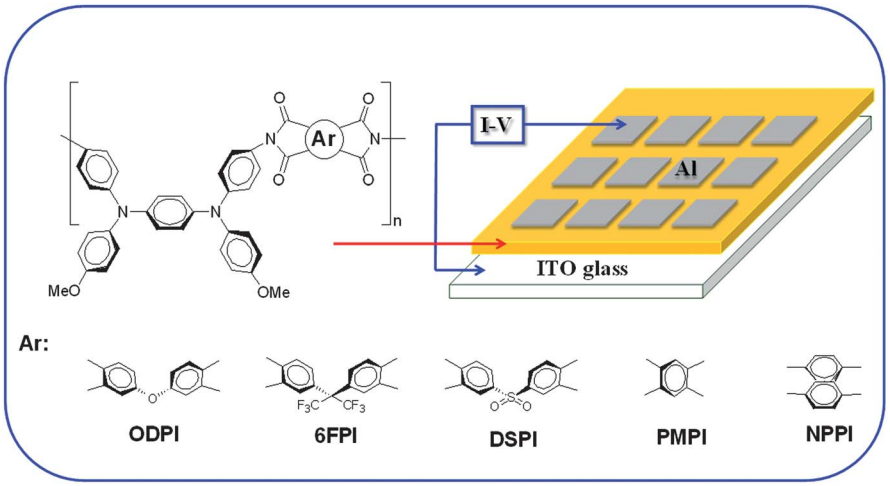

Fig. 1 Molecular structures of TPPA series polyimides and a schematic diagram of the memory device consisting of a polymer thin film sandwiched between an ITO bottom electrode and an Al top electrode.

Optical and electrochemical properties

UV-vis absorption spectra of TPPA series polyimides are shown in Fig. 4 and the onset wavelength of optical absorption were utilized to obtain the optical energy band gap (E_g) of these polyimides. The electrochemical behavior of these polyimides was investigated by cyclic voltammetry conducted using film cast on an ITO-coated glass substrate as the working electrode in dry acetonitrile (CH_3CN) containing 0.1 M of TBAP as an electrolyte under nitrogen atmosphere. The typical cyclic voltammograms for these polyimides are depicted in Fig. 5. There are two reversible oxidation redox couples for all polyimides, and the onset oxidation of these five polyimides exhibited at 0.52, 0.55, 0.58, 0.60, and 0.56 V, respectively. The optical and electrochemical properties of these five polyimides are summarized in Table 4, and the optical energy band gaps (E_g) estimated from the onset optical absorption are 2.36, 2.45, 2.33, 2.30, and

Table 1 Molecular weights[d]

Polymer	η_{inh} (dL g^{-1})	M_w	M_n	PDI[e]	DP[f]
ODPI	0.32[a]	147 100	60 800	2.42	78.5
6FPI	1.08[a]	129 300	62 700	2.06	68.8
DSPI	0.41[a]	79 000	36 200	2.18	43.9
PMPI	0.41[b]	—	—	—	—
NPPI	0.39[c]	—	—	—	—

[a] Measured at a polymer concentration of 0.5 g dL^{-1} in DMAc at 30 °C. [b] Measured at a polymer concentration of 0.5 g dL^{-1} in H_2SO_4 at 30 °C. [c] Measured at a polymer concentration of 0.5 g dL^{-1} in *m*-cresol at 30 °C. [d] Calibrated with polystyrene standards, using NMP as the eluent at a constant flow rate of 0.5 mL min^{-1} at 40 °C. [e] Polydispersity index (M_w/M_n). [f] Degree of polymerization.

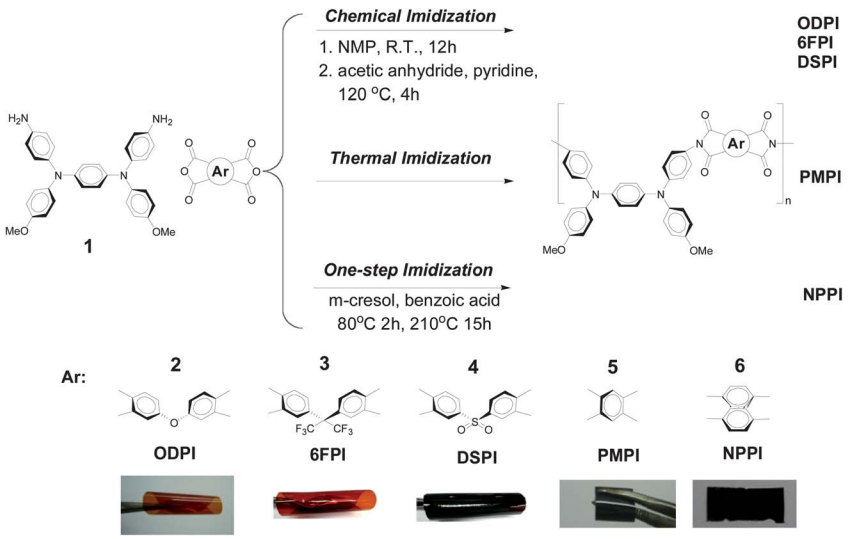

Scheme 1 TPPA series polyimides were prepared by chemical imidization, thermal imidization, and one-step imidization. Photographs show the appearance of these polyimides films (thickness: ~40 μm).

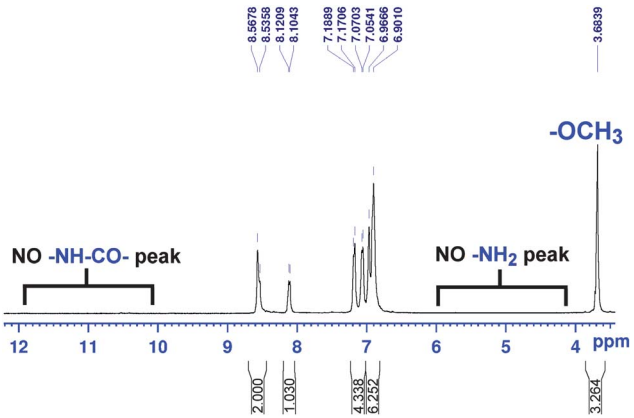

Fig. 2 ^{1}H NMR spectrum of polyimide **DSPI**.

Table 2 Thermal properties

Polymer[a]	T_g[b] (°C)	T_d^5[c] (°C)		T_d^{10}[c] (°C)		R_{w800} (%)[d]
		N_2	Air	N_2	Air	
ODPI	245	490	450	535	510	61
6FPI	287	500	495	530	545	61
DSPI	296	470	460	490	490	57
PMPI	287	525	510	570	560	61
NPPI	284	495	475	520	515	64

[a] The polymer film samples were heated at 300 °C for 1 h prior to all the thermal analyses. [b] Midpoint temperature of baseline shift on the second DSC heating trace (rate: 20 °C min^{-1}) of the sample after quenching from 400 °C to 50 °C (rate: 200 °C min^{-1}) in nitrogen. [c] Temperature at which 5% and 10% weight loss occurred, respectively, recorded by TGA at a heating rate of 20 °C min^{-1} and a gas flow rate of 20 cm^3 min^{-1}. [d] Residual weight percentages at 800 °C under nitrogen flow.

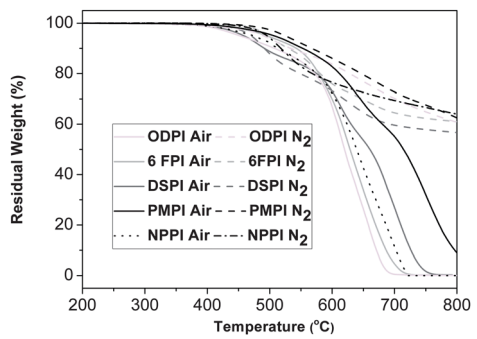

Fig. 3 TGA thermograms of TPPA series polyimides.

2.16 eV, respectively. The lowest energy gap of **NPPI** was an evidence for the strongest charge-transfer effect than other four polyimides. The LUMO energy levels of these polyimides decrease with the dianhydrides electron-withdrawing ability increasing, and are in the order of **ODPI**, **6FPI**, **DSPI**, **PMPI**, and **NPPI**. Furthermore, **ODPI** also revealed lowest onset oxidation potential (0.52 V) than other polyimides because of the weaker electron-withdrawing ability from the dianhydride moiety. The HOMO energy levels of **ODPI**, **6FPI**, **DSPI**, **PMPI**, and **NPPI** estimated from the onset of their oxidation in CV experiments were 4.96, 4.99, 5.02, 5.05, and 5.00 eV, respectively

Table 3 Solubility behavior

Code	Solubility in various solvents[a]						
	NMP	DMAc	DMF	DMSO	*m*-Cresol	THF	$CHCl_3$
ODPI	++	+	+–	+–	++	+–	++
6FPI	++	++	++	+	++	++	++
DSPI	++	++	++	+	+	+–	++
PMPI	+–	+–	–	–	+–	–	+–
NPPI	+–	+–	–	+–	+	+–	+–

[a] The solubility was determined with a 10 mg sample in 1 mL of a solvent. ++, soluble at room temperature; +, soluble on heating at 70–80 °C; +–, partially soluble or swelling; –, insoluble even on heating.

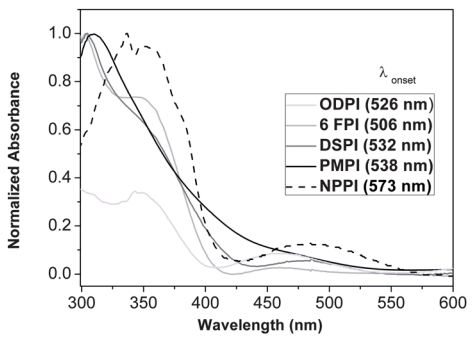

Fig. 4 UV-visible absorption spectra of TPPA series polyimides.

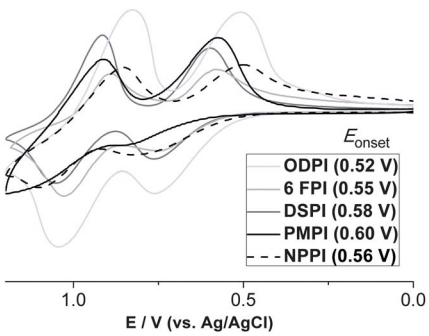

Fig. 5 Cyclic voltammetric diagrams of polymer TPPA series polyimides films on an ITO-coated glass substrate over cyclic scans.

(on the basis of ferrocene/ferrocenium 4.8 eV below the vacuum level with $E_{onset} = 0.36$ V (ref. 12)).

Memory device characteristics of these polyimides

The memory behaviors of these polyimides were depicted by the current–voltage (*I–V*) characteristics of an ITO/polymer/Al sandwich device as shown in Fig. 6. Within the sandwich device, polymer film was used as an active layer between Al and ITO as the top and bottom electrodes. To exclude the effect of the polymer film thickness on memory properties, a standard thickness (50 nm) was used without specific mention. Fig. 6(a) exhibits the *I–V* result of **ODPI**, which was measured with a compliance current of 0.01 A. The memory device of **ODPI** kept at low-conductivity (OFF) state during the positive and

Table 4 Redox potentials and energy levels of polyimides

	UV-vis absorption (nm)		Oxidation potential (V) (*vs.* Ag/AgCl in CH_3CN)					
			$E_{1/2}$[a]					
Polymer	λ_{max}	λ_{onset}	1st	2nd	E_{onset}	E_g[b] (eV)	HOMO[c] (eV)	LUMO (eV)
ODPI	298	526	0.64	0.94	0.52	2.36	4.96	2.60
6FPI	303	506	0.66	0.96	0.55	2.45	4.99	2.61
DSPI	305	532	0.68	0.98	0.58	2.33	5.02	2.69
PMPI	309	538	0.71	1.02	0.60	2.30	5.05	2.75
NPPI	336	573	0.67	0.98	0.56	2.16	5.00	2.84

[a] $E_{1/2}$ (average potential of the redox couple peaks). [b] The data were calculated from polymer films by the equation: $E_g = 1240/\lambda_{onset}$ (energy gap between HOMO and LUMO). [c] The HOMO energy levels were calculated from cyclic voltammetry and were referenced to ferrocene (4.8 eV; onset = 0.36 V).

negative scan. Thus, **ODPI** showed no memory but insulator behavior. *I–V* characteristics of the corresponding **6FPI**[8m] are summarized in Fig. 6(b) as published before. The memory device of **6FPI** switched on from 10^{-13}–10^{-14} to 10^{-5} A at the threshold voltage of −4.6 V in the negative sweep and indicated as volatile DRAM behavior.

Fig. 6(c) and (e) reveal the *I–V* results of DSPI and NPPI. During the first positive sweep from 0 V to 6 V, the device stayed at the OFF state with a current range 10^{-13} to 10^{-14} A, which means that the positive applied voltage could not switch the memory device on. In contrast, during the second negative sweep from 0 V to −6 V, the current increased abruptly from 10^{-13} to

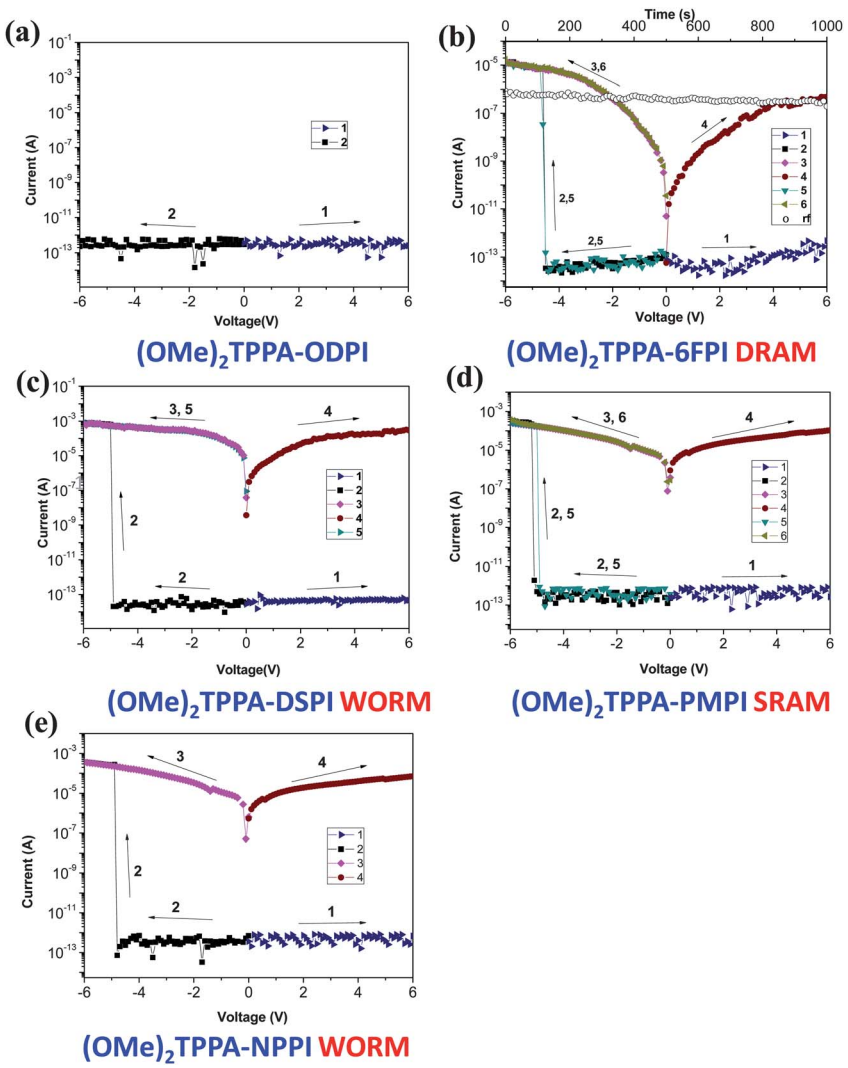

Fig. 6 Current–voltage (*I–V*) characteristics of the ITO/**PI** (50 ± 3 nm)/Al memory device. (a) **ODPI**, (b) **6FPI**, (c) **DSPI**, (d) **PMPI** and (e) **NPPI**.

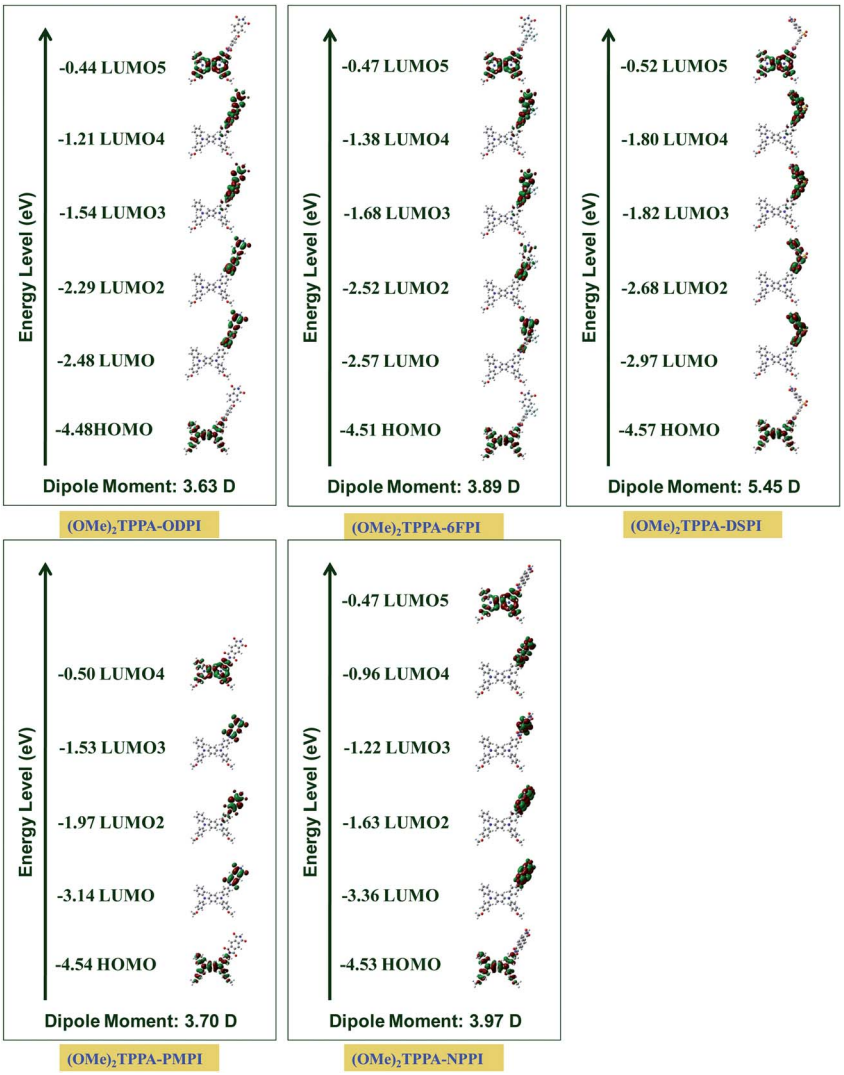

Fig. 7 Calculated molecular orbitals and corresponding energy levels of the basic units (BU) for TPPA series polyimides.

10^{-14} to 10^{-3} A (high-conductivity state) at the threshold voltage of −4.9 V and −4.8 V indicating the transition from the OFF state to high-conductivity (ON) state. In a memory device, this OFF-to-ON transition can be defined as a "writing" process. The device remained at the ON state during the subsequent negative scan (the third sweep) and then positive scan (the fourth sweep). Once DSPI and NPPI memory device has been reached to the ON state, it remains there even after turning off power for 1 h or longer time. These results indicate that the DSPI and NPPI films exhibit non-volatile WORM memory behavior in the device.

Fig. 6(d) depicts the *I*–*V* results of PMPI. The device could not be switched to the ON state and stayed in the OFF state with a current range 10^{-13} in the first positive sweep up to 6 V. However, a sharp increasing of the current could be observed at −5.1 V during the second negative sweep. The device also could remain in the ON state during the subsequent negative (the third sweep) and positive scans (the fourth sweep). Thus, this PMPI memory device could not be reset to the initial OFF state by the introduction of a reverse scan and is thus non-erasable. The device of PMPI maintained in the ON state after turning off the power for a longer period of time than 6FPI. The fifth sweep was conducted after turning off the power for about 11 minutes; it was found that the ON state had relaxed to the steady OFF state without an erasing process. During the fifth sweep, the device could be switched to the ON state again at the threshold voltage of −5.0 V, and the sixth sweep was conducted to make sure the device could open to the ON state again. The longer retention time at the ON state yet volatile, as well as the randomly accessible ON and OFF states is similar to the data remanence behavior of SRAM.[8i]

Comparing to the volatile DRAM nature of **6FPI** published before, the four polyimides synthesized in this study exhibited not only diverse memory properties but also higher ON/OFF current ratios of 10^9 to 10^{10} than that of **6FPI** (10^7). The increased ON/OFF current ratio is advantageous to reduce the probability of misreading between the ON state and the OFF state.

Theoretical analysis and switching mechanism

In order to get more insight into the different memory behavior of the present polyimides devices, molecular simulation on the basic unit was carried out by DFT/B3LYP/6-31G(d) with the

Gaussian 09 program. The charge density isosurfaces of the basic unit, the most energetically favorable geometry, and dipole moment are summarized in Fig. 7. The LUMO energy levels calculated by molecular simulation were in agreement with the experimental values tendency and could be utilized as evidence to indicate the electron-withdrawing intensity of different dianhydrides. For these TPPA polyimides systems, the HOMO energy levels were located mainly at the electron-donating TPPA moieties, while the LUMO energy levels were located at the electron-withdrawing phthalimide units. According to previous literature,[8b,h,i,k] when the applied electric fields reach the switching-on voltage, some electrons at the HOMO accumulate energy and transit to the LUMO5 (LUMO4 for **PMPI**) with the highest probability because of overlapping of the HOMO and LUMO5 resulting in an excited state. Thus, the energy band gap between HOMO and the lowest LUMO5 of electron-donating moiety is one of the important factors for switching-on voltage, and should be very related to the switching-on voltage of memory device. Nevertheless, electrons at the HOMO may also be excited to the three intermediate LUMOs with lower energy barrier belonging to the acceptor units. Thus, charge transfer occurs through several courses to form the conductive charge transfer complexes: indirectly from the LUMO5 through intermediate LUMOs and then to the LUMO, or from the intermediate LUMOs to the LUMO, and directly from the HOMO to the LUMO. When the intra- or intermolecular charge transfer occurred by the applied electric field, the generating holes can be delocalized to the conjugated TPPA moieties forming an open channel in the HOMO of polyimides for the charge carriers (holes) to migrate through. Therefore, the current increases rapidly and the memory device can be switched to the high conductivity state (ON state). Based on this proposed mechanism, when the negative sweep was conducted, the hole injected from the bottom electrode ITO to the HOMO of polymer,[13] thus the lower energy level HOMO of **DSPI**, **PMPI**, and **NPPI** effectively leads to larger energy barrier, resulting in a higher switching-on voltage of these three polyimides than **6FPI** one.

The LUMO energy level of polyimides is very important for the retention time; because the charge transfer complex is a metastable complex, thus the lower LUMO values should make it more stable and keep for longer time. Among these five polyimides, **ODPI** has the largest energy band gap and the weakest charge-transfer capability which result in no memory properties. Comparing to the DRAM behavior of **6FPI**, the lower LUMO energy level of **PMPI** bring about the longer retention time and indicated as SRAM property. The lowest LUMO energy level and the strongest charge-transfer effect of **NPPI** produce the non-volatile WORM behavior. Interestingly, although **DSPI** have the higher LUMO energy level than **PMPI**, it has the non-volatile WORM behavior in place of the volatile properties. The main difference between these two polyimides is the higher dipole moment of **DSPI** (5.45 D) than **PMPI** (3.70 D). According to previous literature,[1c,8j,k] the higher dipole moment brought about the non-volatile memory properties.

Conclusion

In summary, new functional polyimides **ODPI**, **DSPI**, **PMPI**, and **NPPI** have been successfully synthesized for memory device applications. For comparison, the corresponding **6FPI** with different electron-withdrawing capability was also added into the discussion. The memory devices with the configuration of ITO/polyimides/Al exhibited various memory characteristics. **ODPI** didn't have memory properties, **6FPI** exhibited DRAM characteristics, and **PMPI** with the stronger electron-withdrawing moiety revealed SRAM behavior. **NPPI** with the strongest electron-withdrawing unit showed WORM type non-volatile memory behavior. Interestingly, **DSPI**, which has higher LUMO energy level than **PMPI**, manifested non-volatile WORM behavior resulting from the highest dipole moment of 5.45 D. By this facile choice of different kinds of dianhydrides (electron accepters), the resulting polyimides with entirely different memory properties could be readily obtained.

Experimental

Materials

N,*N*′-Bis(4-aminophenyl)-*N*,*N*′-di(4-methoxylphenyl)-1,4-phenylenediamine (**1**) was synthesized according to the previously reported procedure.[11] 2,2-Bis(3,4-dicarboxyphenyl)hexafluoropropane dianhydride (6FDA) (**3**) (Chriskev) and 1,4,5,8-naphthalenetetracarboxylic dianhydrides (NPDA) (**6**) (TCI) were purified by vacuum sublimation. Oxydiphthalic dianhydride (ODPA) (**2**) (Chriskev), 3,3′,4,4′-diphenylsulfonetetracarboxylic dianhydride (DSDA) (**4**) (TCI), and pyromellitic dianhydride (PMDA) (**5**) (Chriskev) were purified by recrystallization from acetic anhydride. Tetrabutylammonium perchlorate (TBAP) (ACROS) was recrystallized twice by ethyl acetate under nitrogen atmosphere and then dried in a vacuum prior to use. All other reagents were used as received from commercial sources.

Preparation of polyimides by a two-step method *via* chemical imidization reaction

The synthesis of polyimide **DSPI** was used as an example to illustrate the general synthetic route for **ODPI**, **6FPI**, and **DSPI**. To a solution of 1.01 mmol of diamine (**1**) in 2.8 mL of *N*-methyl-2-pyrrolidinone (NMP), 0.36 g (1.01 mmol) of dianhydride DSDA (**4**) was added in one portion. The mixture was stirred at room temperature overnight (*ca.* 12 h) to afford a viscous poly(amic acid) solution. The poly(amic acid) was subsequently converted to polyimide *via* a chemical imidization process by addition of pyridine 1.0 mL and acetic anhydride 2.0 mL, then the mixture was heated at 120 °C for 4 h to complete imidization. The resulting polymer solution was poured into 300 mL of methanol giving a fibrous precipitate washed thoroughly with methanol. Reprecipitations of the polymer by DMAc–methanol were carried out for further purification. The inherent viscosity of **DSPI** was 0.41 dL g^{-1} in DMAc at a concentration of 0.5 g dL^{-1} at 30 °C. The weight-average molecular weights (M_w) and polydispersity index of **DSPI** was 79 000 and 2.18, respectively, relative to polystyrene standards.

Preparation of polyimide PMPI by two-step method *via* thermal imidization reaction

To a solution of 1 mmol of diamine (**1**) in 3 mL of *N*,*N*-dimethylacetamide (DMAc), 0.22 g (1 mmol) of dianhydride PMDA

(**5**) was added in one portion. The mixture was stirred at −15 °C for 1 h and r.t. for 2 h to afford a viscous poly(amic acid) (PAA) solution. The poly(amic acid) was subsequently converted to polyimide film *via* a thermal imidization process (100 °C 1 h, 200 °C 1 h, and 300 °C 1 h) in vacuum oven. The inherent viscosity of **PMPI** was 0.41 dL g^{-1} in H_2SO_4 at a concentration of 0.5 g dL^{-1} at 30 °C.

Preparation of polyimide NPPI by one-step method

The stoichiometric mixture of diamine (**1**) (0.82 mmol), dianhydride NPDA (**6**) (0.82 mmol, 0.22 g), and benzoic acid (0.40 g) in 4 mL of *m*-cresol were stirred at 80 °C under nitrogen. After the solution was stirred for 2 h, it was heated to 210 °C for 15 h, and the water produced from imidization was allowed to remove along with *m*-cresol. The obtained polymer solution was poured slowly into 300 mL of stirred methanol giving rise to a fibrous precipitate that was collected by filtration, washed thoroughly with methanol, and dried under vacuum at 100 °C. Reprecipitations of the polymer by *m*-cresol–methanol were carried out for further purification. The inherent viscosity of **NPPI** was 0.39 dL g^{-1} in *m*-cresol at a concentration of 0.5 g dL^{-1} at 30 °C.

Polymer properties measurements

^{1}H NMR spectra were measured on a Bruker AC-300 MHz spectrometer in DMSO-d_6, using tetramethylsilane as an internal reference, and peak multiplicity was reported as follows: s, singlet; d, doublet; m, multiplet. The inherent viscosities were determined at 0.5 g dL^{-1} concentration using Tamson TV-2000 viscometer at 30 °C. Gel permeation chromatographic (GPC) analysis was carried out on a Waters chromatography unit interfaced with a Waters 2410 refractive index detector. Two Waters 5 μm Styragel HR-2 and HR-4 columns (7.8 mm I. D. × 300 mm) were connected in series with NMP as the eluent at a flow rate of 0.5 mL min^{-1} at 40 °C and were calibrated with polystyrene standards. Thermogravimetric analysis (TGA) was conducted with a PerkinElmer Pyris 1 TGA. Experiments were carried out on approximately 3–5 mg film samples heated in flowing nitrogen or air (flow rate = 20 cm^3 min^{-1}) at a heating rate of 20 °C min^{-1}. DSC analyses were performed on a PerkinElmer Pyris 1 DSC at a scan rate of 10 °C min^{-1} in flowing nitrogen (20 cm^3 min^{-1}). Electrochemistry was performed with a CH Instruments 611B electrochemical analyzer. Voltammograms were presented with the positive potential pointing to the left and with increasing anodic currents pointing downwards. Cyclic voltammetry (CV) was conducted with a three-electrode cell in which ITO (polymer films area about 0.5 cm × 1.1 cm) was used as a working electrode. A platinum wire was used as an auxiliary electrode. All cell potentials were taken by using a homemade Ag/AgCl, KCl (sat.) reference electrode. UV-visible absorption was recorded on UV-visible spectrophotometer (Hitachi U-4100).

Fabrication and measurement of the memory device

The memory device was fabricated with the configuration of ITO/polymer/Al as shown in Fig. 1. The ITO glass used for the memory device was pre-cleaned by ultrasonication with water, acetone, and isopropanol, each for 15 min. The solution of **6FPI**, **DSPI**, **ODPI**, and **NPPI** (20 mg mL^{-1} in *m*-cresol for **NPPI**, 25 mg mL^{-1} in DMAc for others) was first filtered through 0.45 μm pore size of PTFE membrane syringe filter. Then, 250 μL of the filtered solution was spin-coated onto the ITO glass at a rotation rate of 1000 rpm for 60 s and kept at 100 °C for 10 min under nitrogen (150 °C for **NPPI**). **PMPI** memory device was prepared by PAA solution and then thermal imidization was performed as mentioned above. The thickness of thin films was determined by alpha-step profilometer. A 300 nm thick Al top electrode was thermally evaporated through the shadow mask (recorded device units of 0.5 × 0.5 mm^2 in size) at a pressure of 10^{-7} torr with a uniform depositing rate of 3–6 Å s^{-1}. The electrical characterization of the memory device was performed by a Keithley 4200-SCS semiconductor parameter analyzer equipped with a Keithely 4205-PG2 arbitrary waveform pulse generator. ITO was used as common electrode and Al was the electrode for applying voltage during the sweep.

Molecular simulation

Molecular simulations in this study were carried out with the Gaussian 09 program package. Equilibrium ground state geometry and electronic properties of basic unit of TPPA series polyimides were optimized by means of the density functional theory (DFT) method at the B3LYP level of theory (Beckesstyle three-parameter density functional theory using the Lee–Yang–Parr correlation functional) with the 6-31G(d) basic set.

Acknowledgements

We gratefully acknowledge the financial support of this research through the National Science Council of Taiwan. C. W. Lu at the Instrumentation Center, National Taiwan University, for CHNS (EA) analysis experiments and C. H. Ho at the Instrumentation Center, Department of Chemistry, National Taiwan Normal University, for the measurement of 500 MHz NMR spectrometer are also acknowledged.

References and notes

1 (*a*) Y. Yang, J. Ouyang, L. P. Ma, R. J. H. Tseng and C. W. Chu, *Adv. Funct. Mater.*, 2006, **16**, 1001; (*b*) S. Baek, D. Lee, J. Kim, S. H. Hong, O. Kim and M. Ree, *Adv. Funct. Mater.*, 2007, **17**, 2637; (*c*) Q. D. Ling, D. J. Liaw, E. Y. H. Teo, C. X. Zhu, D. S. H. Chan, E. T. Kang and K. G. Neoh, *Polymer*, 2007, **48**, 5182; (*d*) Q. D. Ling, D. J. Liaw, C. X. Zhu, D. S. H. Chan, E. T. Kang and K. G. Neoh, *Prog. Polym. Sci.*, 2008, **33**, 917; (*e*) T. J. Lee, S. Park, S. G. Hahm, D. M. Kim, K. Kim, J. Kim, W. Kwon, Y. Kim, T. Chang and M. Ree, *J. Phys. Chem. C*, 2009, **113**, 3855; (*f*) G. Liu, Q. D. Ling, E. Y. H. Teo, C. X. Zhu, D. S. H. Chan, K. G. Neoh and E. T. Kang, *ACS Nano*, 2009, **3**, 1929; (*g*) Y. K. Fang, C. L. Liu, C. X. Li, C. J. Lin, R. Mezzenga and W. C. Chen, *Adv. Funct. Mater.*, 2010, **20**, 3012; (*h*) S. Park, T. J. Lee, D. M. Kim, J. C. Kim, K. Kim, W. Kwon, Y. G. Ko, H. Choi, T. Chang and M. Ree, *J. Phys. Chem. B*, 2010, **114**, 10294; (*i*) X. D. Zhuang, Y. Chen, G. Liu, B. Zhang, K. G. Neoh, E. T. Kang, C. X. Zhu, Y. X. Li and L. J. Niu, *Adv. Funct. Mater.*, 2010, **20**, 2916; (*j*) P. O. Sliva, G. Dir and C. Griffiths, *J. Non-Cryst. Solids*, 1970, **2**, 316; (*k*) C. Wu, F. Li, Y. Zhang, T. Guo and T. Chen, *Appl. Phys. Lett.*, 2011, **99**; (*l*) B. Koo, H. Baek and J. Cho, *Chem. Mater.*, 2012, **24**, 1091; (*m*) J. E. Park, J. H. Eom, T. Lim, D. H. Hwang and S. Pyo, *J. Polym. Sci., Part A: Polym. Chem.*, 2012, **50**, 2188; (*n*) S. J. Liu, Z. H. Lin, Q. Zhao, Y. Ma, H. F. Shi, M. D. Yi, Q. D. Ling, Q. L. Fan, C. X. Zhu, E. T. Kang and W. Huang, *Adv. Funct. Mater.*, 2011, **21**, 979; (*o*) P. Wang,

S. J. Liu, Z. H. Lin, X. C. Dong, Q. Zhao, W. P. Lin, M. D. Yi, S. H. Ye, C. X. Zhu and W. Huang, *J. Mater. Chem.*, 2012, **22**, 9576; (*p*) S. J. Liu, Y. Chang, W. J. Xu, Q. Zhao and W. Huang, *Macromol. Rapid Commun.*, 2012, **33**, 461.

2 (*a*) R. H. Friend, R. W. Gymer, A. B. Holmes, J. H. Burroughes, R. N. Marks, C. Taliani, D. D. C. Bradley, D. A. Dos Santos, J. L. Bredas, M. Logdlund and W. R. Salaneck, *Nature*, 1999, **397**, 121; (*b*) K. Lee, J. Y. Kim, S. H. Park, S. H. Kim, S. Cho and A. J. Heeger, *Adv. Mater.*, 2007, **19**, 2445; (*c*) Y. Shao, G. C. Bazan and A. J. Heeger, *Adv. Mater.*, 2008, **20**, 1191; (*d*) Y. Shao, X. Gong, A. J. Heeger, M. Liu and A. K. Y. Jen, *Adv. Mater.*, 2009, **21**, 1972.

3 (*a*) H. Sirringhaus, N. Tessler and R. H. Friend, *Science*, 1998, **280**, 1741; (*b*) T. Yamamoto, H. Kokubo, M. Kobashi and Y. Sakai, *Chem. Mater.*, 2004, **16**, 4616; (*c*) L. L. Chua, J. Zaumseil, J. F. Chang, E. C. W. Ou, P. K. H. Ho, H. Sirringhaus and R. H. Friend, *Nature*, 2005, **434**, 194; (*d*) A. Babel, Y. Zhu, K. F. Cheng, W. C. Chen and S. A. Jenekhe, *Adv. Funct. Mater.*, 2007, **17**, 2542; (*e*) M. Morana, P. Koers, C. Waldauf, M. Koppe, D. Muehlbacher, P. Denk, M. Scharber, D. Waller and C. Brabec, *Adv. Funct. Mater.*, 2007, **17**, 3274; (*f*) M. Morana, M. Wegscheider, A. Bonanni, N. Kopidakis, S. Shaheen, M. Scharber, Z. Zhu, D. Waller, R. Gaudiana and C. Brabec, *Adv. Funct. Mater.*, 2008, **18**, 1757; (*g*) H. Yan, Z. H. Chen, Y. Zheng, C. Newman, J. R. Quinn, F. Dotz, M. Kastler and A. Facchetti, *Nature*, 2009, **457**, 679; (*h*) J. H. Tsai, W. Y. Lee, W. C. Chen, C. Y. Yu, G. W. Hwang and C. Ting, *Chem. Mater.*, 2010, **22**, 3290.

4 (*a*) G. Yu, J. Gao, J. C. Hummelen, F. Wudl and A. J. Heeger, *Science*, 1995, **270**, 1789; (*b*) C. J. Brabec, N. S. Sariciftci and J. C. Hummelen, *Adv. Funct. Mater.*, 2001, **11**, 15; (*c*) G. Li, V. Shrotriya, J. S. Huang, Y. Yao, T. Moriarty, K. Emery and Y. Yang, *Nat. Mater.*, 2005, **4**, 864; (*d*) M. H. Chen, J. Hou, Z. Hong, G. Yang, S. Sista, L. M. Chen and Y. Yang, *Adv. Mater.*, 2009, **21**, 4238; (*e*) J. H. Hou, T. L. Chen, S. Q. Zhang, L. J. Huo, S. Sista and Y. Yang, *Macromolecules*, 2009, **42**, 9217; (*f*) A. Kumar, H. H. Liao and Y. Yang, *Org. Electron.*, 2009, **10**, 1615; (*g*) L. J. Huo, J. H. Hou, S. Q. Zhang, H. Y. Chen and Y. Yang, *Angew. Chem., Int. Ed.*, 2010, **49**, 1500; (*h*) S. Sista, Z. R. Hong, M. H. Park, Z. Xu and Y. Yang, *Adv. Mater.*, 2010, **22**, E77.

5 A. Stikeman, *Technol. Rev.*, 2002, 31.

6 C. Lee, I. Kim, H. Shin, S. Kim and J. Cho, *Langmuir*, 2009, **25**, 11276.

7 (*a*) H. T. Lin, Z. W. Pei, J. R. Chen, G. W. Hwang, J. F. Fan and Y. J. Chan, *IEEE Electron Device Lett.*, 2007, **28**, 951; (*b*) A. Laiho, H. S. Majumdar, J. K. Baral, F. Jansson, R. Osterbacka and O. Ikkala, *Appl. Phys. Lett.*, 2008, **93**, 2003309; (*c*) G. Liu, Q. D. Ling, E. T. Kang, K. G. Neoh, D. J. Liaw, F. C. Chang, C. X. Zhu and D. S. H. Chan, *J. Appl. Phys.*, 2007, **102**; (*d*) R. J. Tseng, J. X. Huang, J. Ouyang, R. B. Kaner and Y. Yang, *Nano Lett.*, 2005, **5**, 1077; (*e*) J. Y. Ouyang, C. W. Chu, R. J. H. Tseng, A. Prakash and Y. Yang, *Proc. IEEE*, 2005, **93**, 1287; (*f*) J. Y. Ouyang, C. W. Chu, C. R. Szmanda, L. P. Ma and Y. Yang, *Nat. Mater.*, 2004, **3**, 918.

8 (*a*) S. H. Cheng, S. H. Hsiao, T. X. Su and G. S. Liou, *Macromolecules*, 2005, **38**, 307; (*b*) Q. D. Ling, F. C. Chang, Y. Song, C. X. Zhu, D. J. Liaw, D. S. H. Chan, E. T. Kang and K. G. Neoh, *J. Am. Chem. Soc.*, 2006, **128**, 8732; (*c*) S. G. Hahm, S. Choi, S. H. Hong, T. J. Lee, S. Park, D. M. Kim, W. S. Kwon, K. Kim, O. Kim and M. Ree, *Adv. Funct. Mater.*, 2008, **18**, 3276; (*d*) S. G. Hahm, S. Choi, S. H. Hong, T. J. Lee, S. Park, D. M. Kim, J. C. Kim, W. Kwon, K. Kim, M. J. Kim, O. Kim and M. Ree, *J. Mater. Chem.*, 2009, **19**, 2207; (*e*) D. M. Kim, S. Park, T. J. Lee, S. G. Hahm, K. Kim, J. C. Kim, W. Kwon and M. Ree, *Langmuir*, 2009, **25**, 11713; (*f*) K. Kim, S. Park, S. G. Hahm, T. J. Lee, D. M. Kim, J. C. Kim, W. Kwon, Y. G. Ko and M. Ree, *J. Phys. Chem. B*, 2009, **113**, 9143; (*g*) T. J. Lee, C. W. Chang, S. G. Hahm, K. Kim, S. Park, D. M. Kim, J. Kim, W. S. Kwon, G. S. Liou and M. Ree, *Nanotechnology*, 2009, **20**, 135204; (*h*) Y. L. Liu, Q. D. Ling, E. T. Kang, K. G. Neoh, D. J. Liaw, K. L. Wang, W. T. Liou, C. X. Zhu and D. S. H. Chan, *J. Appl. Phys.*, 2009, **105**; (*i*) Y. L. Liu, K. L. Wang, G. S. Huang, C. X. Zhu, E. S. Tok, K. G. Neoh and E. T. Kang, *Chem. Mater.*, 2009, **21**, 3391; (*j*) N. H. You, C. C. Chueh, C. L. Liu, M. Ueda and W. C. Chen, *Macromolecules*, 2009, **42**, 4456; (*k*) T. Kuorosawa, C. C. Chueh, C. L. Liu, T. Higashihara, M. Ueda and W. C. Chen, *Macromolecules*, 2010, **43**, 1236; (*l*) K. L. Wang, Y. L. Liu, J. W. Lee, K. G. Neoh and E. T. Kang, *Macromolecules*, 2010, **43**, 7159; (*m*) C. J. Chen, H. J. Yen, W. C. Chen and G. S. Liou, *J. Polym. Sci., Part A: Polym. Chem.*, 2011, **49**, 3709; (*n*) Y. Q. Li, R. C. Fang, A. M. Zheng, Y. Y. Chu, X. Tao, H. H. Xu, S. J. Ding and Y. Z. Shen, *J. Mater. Chem.*, 2011, **21**, 15643; (*o*) Y. Q. Li, R. C. Fang, S. J. Ding and Y. Z. Shen, *Macromol. Chem. Phys.*, 2011, **212**, 2360; (*p*) Y. Q. Li, H. H. Xu, X. Tao, K. J. Qian, S. Fu, S. J. Ding and Y. Z. Shen, *Polym. Int.*, 2011, **60**, 1679; (*q*) Y. Zhang, Y. W. Liu, Q. Lan, S. W. Liu, Z. X. Qin, L. H. Chen, C. Y. Zhao, Z. G. Chi, J. R. Xu and J. Economy, *Chem. Mater.*, 2012, **24**, 1212; (*r*) B. L. Hu, F. Zhuge, X. J. Zhu, S. S. Peng, X. X. Chen, L. Pan, Q. Yan and R. W. Li, *J. Mater. Chem.*, 2012, **22**, 520; (*s*) Y. Q. Li, Y. Y. Chu, R. C. Fang, S. J. Ding, Y. L. Wang, Y. Z. Shen and A. M. Zheng, *Polymer*, 2012, **53**, 229; (*t*) D. M. Kim, Y. G. Ko, J. K. Choi, K. Kim, W. Kwon, J. Jung, T. H. Yoon and M. Ree, *Polymer*, 2012, **53**, 1703.

9 (*a*) D. Ma, M. Aguiar, J. A. Freire and I. A. Hummelgen, *Adv. Mater.*, 2000, **12**, 1063; (*b*) S. L. Lim, Q. Ling, E. Y. H. Teo, C. X. Zhu, D. S. H. Chan, E. T. Kang and K. G. Neoh, *Chem. Mater.*, 2007, **19**, 5148; (*c*) H. S. Majumdar, A. Bandyopadhyay, A. Bolognesi and A. J. Pal, *J. Appl. Phys.*, 2002, **91**, 2433; (*d*) E. Y. H. Teo, Q. D. Ling, Y. Song, Y. P. Tan, W. Wang, E. T. Kang, D. S. H. Chan and C. Zhu, *Org. Electron.*, 2006, **7**, 173.

10 (*a*) G. S. Liou, S. H. Hsiao and T. X. Su, *J. Mater. Chem.*, 2005, **15**, 1812; (*b*) C. W. Chang, G. S. Liou and S. H. Hsiao, *J. Mater. Chem.*, 2007, **17**, 1007; (*c*) C. W. Chang and G. S. Liou, *J. Mater. Chem.*, 2008, **18**, 5638; (*d*) G. S. Liou and C. W. Chang, *Macromolecules*, 2008, **41**, 1667; (*e*) S. H. Hsiao, G. S. Liou, Y. C. Kung and H. J. Yen, *Macromolecules*, 2008, **41**, 2800; (*f*) H. J. Yen, H. Y. Lin and G. S. Liou, *Chem. Mater.*, 2011, **23**, 1874; (*g*) H. J. Yen, K. Y. Lin and G. S. Liou, *J. Mater. Chem.*, 2011, **21**, 6230; (*h*) L. T. Huang, H. J. Yen, C. W. Chang and G. S. Liou, *J. Polym. Sci., Part A: Polym. Chem.*, 2010, **48**, 4747; (*i*) S. H. Hsiao, G. S. Liou and H. M. Wang, *J. Polym. Sci., Part A: Polym. Chem.*, 2009, **47**, 2330; (*j*) H. W. Chang, K. H. Lin, C. C. Chueh, G. S. Liou and W. C. Chen, *J. Polym. Sci., Part A: Polym. Chem.*, 2009, **47**, 4037; (*k*) G. S. Liou, H. J. Yen and M. C. Chiang, *J. Polym. Sci., Part A: Polym. Chem.*, 2009, **47**, 5378.

11 H. J. Yen and G. S. Liou, *Chem. Mater.*, 2009, **21**, 4062.

12 G. Gritzner and J. Kutta, *Pure Appl. Chem.*, 1984, **56**, 461.

13 Q. D. Ling, Y. Song, S. L. Lim, E. Y. H. Teo, Y. P. Tan, C. X. Zhu, D. S. H. Chan, D. L. Kwong, E. T. Kang and K. G. Neoh, *Angew. Chem., Int. Ed.*, 2006, **45**, 2947.